Agricultural Systems 171 (2019) 76–88

Contents lists available at ScienceDirect

Agricultural Systems

journal homepage: www.elsevier.com/locate/agsy

Economy-wide climate change impacts on green water droughts based on the hydrologic simulations

Hyunwoo Kang[a], Venkataramana Sridhar[a,*], Bradford F. Mills[b], W. Cully Hession[a], Jactone A. Ogejo[a]

[a] Department of Biological Systems Engineering, Virginia Polytechnic Institute and State University, Blacksburg, Virginia 24061, USA
[b] Department of Agricultural and Applied Economics, Virginia Polytechnic Institute and State University, Blacksburg, Virginia 24061, USA

ARTICLE INFO

Keywords:
Soil moisture
Drought
Climate change
Agricultural production
Economic impacts

ABSTRACT

The impacts of climate change on green water drought and associated economic activity can be simulated with future climate projections, hydrologic models that predict drought indices based on reliable soil moisture, and historic relationships between drought indices and agricultural sector impacts. This study compares the potential impacts of climate change on future agricultural drought and economic conditions in a rural and an urban congressional district in Northern Virginia (VA). The Variable Infiltration Capacity (VIC) model is applied to estimate a soil moisture index (SSI), which is then employed with historic and future climate data to generate SSI predictions. Economic impacts of future SSI changes are inferred from linear regression analysis of the historic relationship between annual mean SSI values and agricultural production values for a seven-year period (2010–2016). The two districts face similar future temperature and precipitation changes due to geographic proximity, but soil moisture, agricultural production and economy-wide responses to climate change differ considerably due to differences in land use and economic structure. In the more rural district, the mean value of drought occurrence increases 38%, while in the more urban district the increase is only 15%. Similarly, economy-wide agricultural sector value added decreases between 17% and 22% in the rural district and between 1 and 5% in the urban district. More studies are required to understand the impacts of adaption on agricultural and other economic sectors both rural and urban regions. More research should be carried out with an application of blue water droughts that have significant impacts to explain the economic impact of droughts.

1. Introduction

Drought is an unpredictable hydrometeorological event, which generates a notable decrease in water resources affecting a large area. Droughts often generated considerable economic losses (CHJ, 2007; Pauw et al., 2011; Faust et al., 2015; Ziolkowska, 2016; Freire-González et al., 2017a), and several studies identified the methods and frameworks for estimating the economic impacts of droughts (Ding et al., 2011; Logar and van den Bergh, 2013; Freire-González et al., 2017b). In many regions, climate change is projected to alter water management practices (Hoekema and Sridhar, 2013) and increase the frequency and severity of droughts (Dai, 2011; Thilakarathne and Sridhar, 2017). Also, the recent Intergovernmental Panel on Climate Change (IPCC) documents that the frequency and severity of drought would likely increase by the end of the 21st century due to the precipitation deficits during the dry seasons (IPCC, 2014). In fact, the United States (US), the severity of droughts increased significantly in the last several decades (Karl et al., 2012), and climate models suggest that changes in precipitation and temperature patterns will lead to even higher frequency and longer duration of droughts in many areas (Seager et al., 2007; Wuebbles et al., 2014; Kang and Sridhar, 2017; Kang and Sridhar, 2018). Future changes in hydrometeorological conditions will influence the US economy. Ample evidence exists that drought has negative impacts on the agricultural sector of the economy. For example, the economic impact of the widespread 1988 drought in the Mid-Atlantic, Southeastern, Midwestern, and Northern Great Plains regions of the US was estimated at $40 billion (Riebsame et al., 1990). At the state level, economic losses of $7.62 billion were estimated in Texas's agricultural sector from 2011 drought (Combs, 2012; Guerrero, 2012), and economic losses of $5.5 billion were estimated in the California agricultural sector from 2014 to 2016 drought (Howitt et al., 2014; Howitt et al., 2015; Medellín-Azuara et al., 2016).

This study simulates the economic impacts of drought on the agricultural sector. High-resolution and long-term hydrometeorological

* Corresponding author.
E-mail address: vsri@vt.edu (V. Sridhar).

https://doi.org/10.1016/j.agsy.2019.01.006
Received 31 October 2018; Received in revised form 24 December 2018; Accepted 17 January 2019
Available online 29 January 2019
0308-521X/

observations are as often unavailable (Sridhar and Wedin, 2009), but physically based hydrologic models can be employed as a reliable alternative to simulate soil moisture levels associated with climate change projections (Nam et al., 2015; Cheng et al., 2016; Schlaepfer et al., 2017). The Variable Infiltration Capacity model (VIC) (Liang et al., 1994), in particular, applied to estimate the impacts of climate change on the hydrologic cycle and drought conditions through soil moisture simulation (Mishra et al., 2010; Leng et al., 2015).

Numerous studies have analyzed the subsequent impacts of droughts on agricultural production and the agricultural sector economy (Calatrava and Garrido, 2005; Peck and Adams, 2010; Gil Sevilla et al., 2013; Howitt et al., 2015; Ziolkowska, 2016). Bauman et al. (2013) evaluate the direct and indirect impacts of the 2011 drought on rural communities in Colorado using an Equilibrium Displacement Mathematical Programming (EDMP) model. Ziolkowska (2016) analyze the economic implications of Texas's drought for the agricultural sector and broader economy with IMPLAN, a representative input–output (I–O) model. However, economic impacts of future drought projections from physically based hydrologic model have not been generated for Mid-Atlantic areas of the US. In this region, soil moisture has been poorly observed historically, making the VIC model has been a good alternative to generate realistic simulations of soil moisture and drought conditions for the historic and future periods at a high spatial resolution (Cayan et al., 2010). Further, the region is densely populated leading to a high degree of heterogeneity in and over climatically similar areas.

The objective of this study is to evaluate the economic impacts of droughts by assessing drought frequency and severity under present and future conditions using drought indices generated from soil moisture simulations. Specifically, the VIC model is used to simulate soil moisture for historic (1977–2016) and future periods (f1: 2017–2056, f2:2057–2096). A soil moisture-based agricultural drought index (SSI) is then computed for the corresponding periods. Agricultural sector impacts of drought are established by estimating the relationship between historic agricultural production for the 2010–2016 period and the annual mean of the SSI with an Ordinary Least Square (OLS) regression model in two economically diverse congressional districts of VA having high value crops that are diverse in terms of both land use and role of agriculture in the economy. Future impacts of the climate change on the agricultural sector and the wider economy are then examined with the IMPLAN model. The approach demonstrated a relatively low-cost framework to quantify the costs of climate change. However, this study primarily focuses on impacts of droughts on rain-fed agriculture (i.e., Green water; Freire-González et al., 2017b), but the other impact assessments of 'Blue water' (e.g., reservoir operations, groundwater withdrawals) and their flexibility in the system are not considered. The simulation results can be used to improve drought mitigation planning and risk assessment, and to aid in the design of sustainable and efficient water management strategies.

2. Methods

An overview of the approaches and methods applied in the paper is provided in the flow diagram in Fig. 1. First, the required input data to drive the VIC model are prepared at a 1/16-degree resolution (0.0625°; 5–6 km). Atmospheric forcing (daily precipitation, maximum and minimum temperatures, and wind speed) are obtained from Livneh et al. (2013). Other model inputs such as vegetation information and soil parameters are obtained from the Land Data Assimilation Systems (LDAS) (http://ldas.gsfc.nasa.gov/). Second, daily simulations of soil moisture for historical and future periods are performed. Third, a soil moisture-based drought index (SSI) is calculated at a weekly time step, which provides a better indicator for evaluating and managing agricultural drought conditions than monthly or seasonal time steps. Fourth, regression analysis estimates the relationship between the mean annual SSI values and rain-fed agricultural product sector data from the IMPLAN model for the retrospective period (2010–2016) in two congressional districts in Northern VA (VA06 and VA11). The impacts of climate change on the agricultural sector are evaluated by applying SSI - agricultural sector relationships to future climatic conditions. Finally, the impacts of green water droughts on the agricultural sector of the economy under climate change projections are then estimated using the IMPLAN model.

2.1. Study area

The study area consists of two congressional districts located in Northern VA: VA06 and VA11 (Fig. 2). VA06 is composed of the Shenandoah, Rockingham, Augusta, Rockbridge, Amherst, Botetourt, Bath, and Highland counties, and the VA11 contains some areas of Fairfax and Prince William counties. Fig. 2 shows the location, topography, and land-use types of the study area and climate divisions associated with the two districts of VA. Table 1 shows the land-use characteristics of the two congressional districts. In the VA06 district, most of the area is covered by forest (69.9%), while the remainder consists of pasture/hay (19.9%), developed areas (7.8%), and cultivated crops (1.2%). The VA11 district is primarily covered by developed areas (63.0%), with a smaller area covered by forest (25%). The districts, thus, encompass a diversity of climate change impacts on drought and agricultural production through varying economic, land-use, and different hydrologic characteristics in rural and urban areas where the water budgets work differently. In addition, the selected districts overlap with several VA climate divisions (Divisions 3, 4, and 5) (Fig. 2(b)). Climate divisions are developed for national, statewide, regional, and population-weighted monitoring of precipitation, temperature, heating/cooling degree, and drought conditions. In the Contiguous US (CONUS), there are 344 climate divisions, and monthly station data are provided based on the daily observations (ftp://ftp.ncdc.noaa.gov/pub/data).

Fig. 3 shows the time series plots of drought areas in these three climate divisions from the USDM (http://droughtmonitor.unl.edu/; Svoboda et al., 2002). For the periods 2002 to 2003, 2007 to 2008, 2011 to 2012, and 2017, all two districts experienced moderate to extreme droughts that influenced agricultural production and the broader economy (DRTAC, 2003; VDEM, 2013). Future projections for these regions indicate that overall increases in agricultural droughts are expected (Kang and Sridhar, 2017). But the regions face different levels of expense to future droughts due to different land use and different levels of importance of agriculture in their economics, despite close proximate and relatively similar historic exposure to droughts. The agricultural-related gross income in the VA06 district is the highest in Virginia ($30,531,000) (USDA NASS, 2012), as agriculture is an important industry in the region. By contrast, VA11 is located in urbanized areas, and the agricultural-related gross income is among the lowest in Virginia ($316,000).

2.2. VIC and IMPLAN model descriptions

Hydrologic simulations are required to obtain long-term soil moisture and soil moisture-based drought indices for both historic and future periods. The VIC model (Liang et al., 1994) is a macro-scale hydrologic model that computes water and energy budget components on a daily time step. The VIC model has been widely used to estimate the drought conditions of various river basins in the US (Shukla et al., 2011; Mao et al., 2015) as well as the impacts of climate change on drought conditions (Kang and Sridhar, 2018). Land cover in the VIC model is classified by types of bare soil or vegetation, and the soil column is divided into three layers. The hydrologic simulation is computed based on the interactions between vegetation and soil in each grid cell and weather variables, such as daily precipitation and temperature.

In this study, the VIC model is implemented at a 1/16th-degree resolution (0.0625°) with atmospheric variables (daily precipitation,

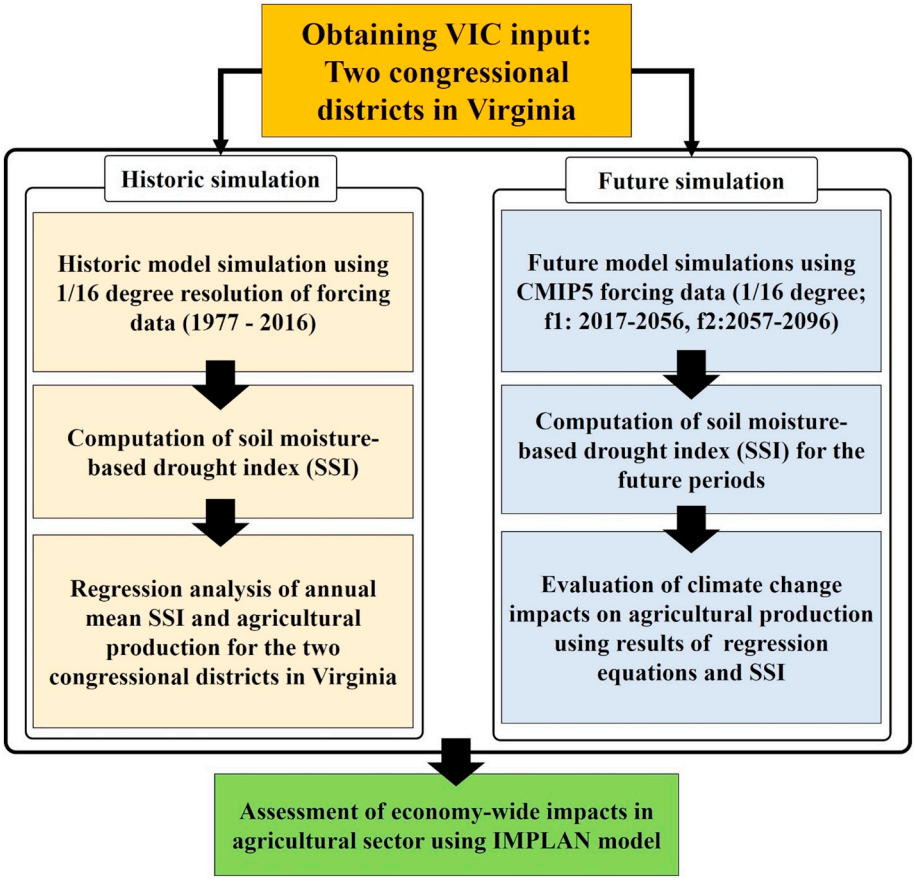

Fig. 1. Flow diagram of overall processes of hydrological modeling, drought projection, and evaluation of climate change effects on economic production. VIC, Variable Infiltration Capacity; CMIP5, Coupled Model Intercomparison Project 5; IMPLAN, IMpact analysis for PLANning.

maximum and minimum temperatures, and wind speed). Other model inputs, such as soil and vegetation data, are obtained for VA06 and VA11 from the Land Data Assimilation Systems (LDAS) (http://ldas.gsfc.nasa.gov/) at the same spatial resolution as the meteorological forcing.

IMPLAN (Minnesota IMPLAN Group, 2009) is a representative Input-Output (I–O) and social accounting matrix model that is applied to evaluate the economy-wide impacts of drought through its direct impacts on agricultural production (Howitt et al., 2014; Howitt et al., 2015; Ziolkowska, 2016). The IMPLAN model relies on datasets from the US Bureau of Economic Analysis (BEA), US Bureau of Labor Statistics (BLS), and US Census Bureau (BOC). Data on the US economy is structured based on the US Census Bureau North American Industry Classification System (NAICS) classification (Table 2). In this study, seven years of annual agricultural production for each sector are provided from the IMPLAN model for the two congressional districts in VA (2010–2016), and they are used to generate a regression analysis of agricultural sector productions and annual mean SSI values. Based on the regression analysis and future SSI, future agricultural production levels are simulated. The IMPLAN then uses projected agricultural production levels to generate economy-wide impacts of drought. The IMPLAN model, specifically generates changes in economic measures of employment, labor income, value added, and industrial output. Table 2 presents the NAICS classification of sectors used to specify direct agricultural production impacts. An additional agricultural sector that relies solely on irrigated fields is excluded from the analysis (e.g., greenhouse production), as direct impacts from droughts are likely to be limited in the sector. However, even the selected sectors are also mixed with green and blue water impacts; this study does not consider the impacts of blue water droughts.

2.3. Analysis of historic and future drought projections

The VIC model is run at a daily time step for the historic period (1977–2016) with three years for the spin-up period (1974–1976), a historic period of 1977–2016, and projected future periods (f1: 2017–2056, f2:2057–2096). For the historic period, the extended and spatially refined long-term hydrologic dataset provided by Livneh et al. (2013) is used at a 1/16th-degree resolution.

For the future simulations, the CMIP5 dataset is used. The CMIP5 projections provide a larger range of potential changes in global precipitation and temperature, and the archive integrates advanced climate models and the recent emission scenarios (Rogelj et al., 2012). CMIP5 consolidates previously ignored factors and more robust processes and properties of the climate systems. The resolution of the CMIP5 dataset is coarse and must be downscaled to a high resolution to correspond to the historic period (1/16th-degree resolution). Thus, we use atmospheric forcing from the two General Circulation Models (GCMs), which were downscaled by the Multivariate Adaptive Constructed Analogs (MACA) method (Abatzoglou, 2013) approach to the VIC model.

The MACA method uses multiple Representative Concentration Pathways (RCPs), and the pathways are commonly used for climate modeling. They demonstrate four possible scenarios, which depends on future greenhouse gas emissions. The four RCPs are named by a range of radiative forcing in the year 2100, and they are RCP2.6, RCP4.5, RCP6, and RCP8.5. In this study, the median (RCP4.5) and highest (RCP8.5) forcing scenarios are employed, which stabilize radiative forcing at 4.5 W/m^2 and 8.5 W/m^2, respectively (Riahi et al., 2011; Thomson et al., 2011). RCP4.5 is a pathway to the stabilization scenario in which total radiative forcing is stabilized shortly after 2100, and

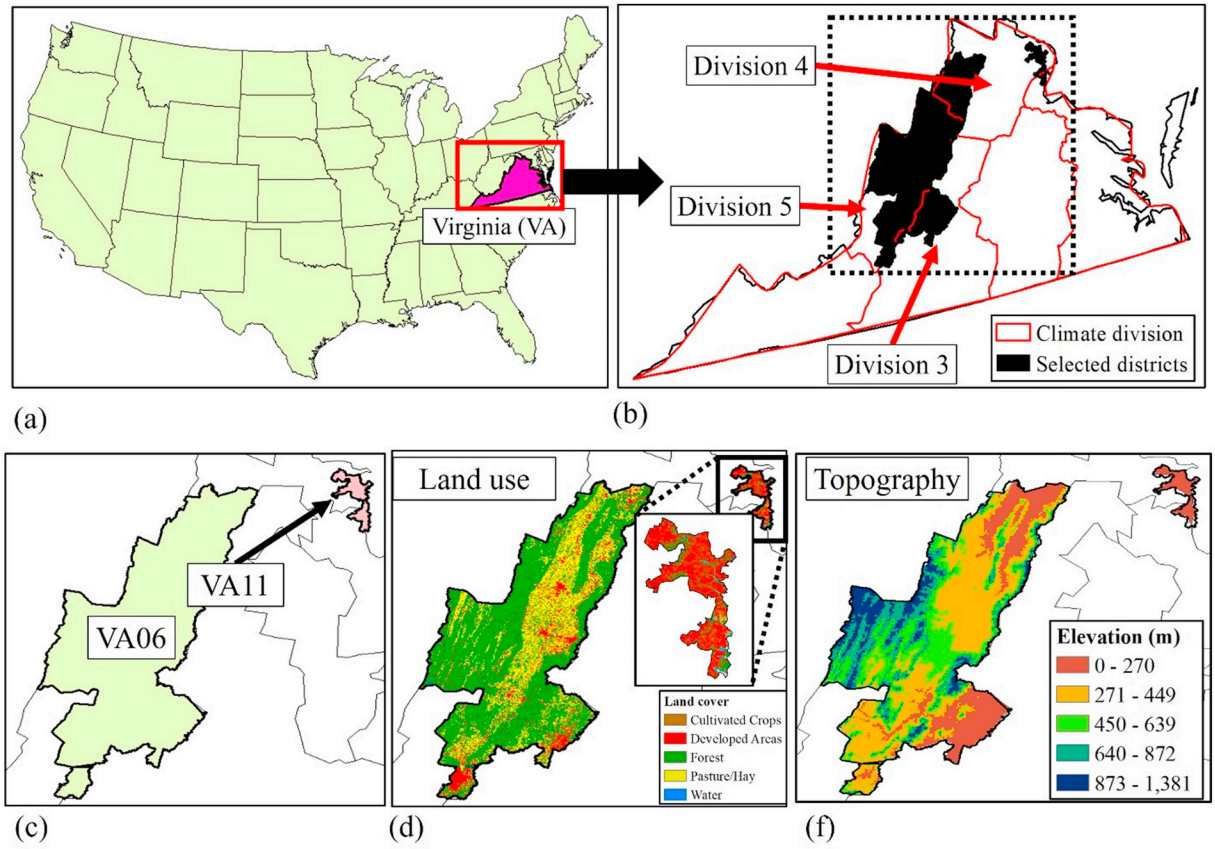

Fig. 2. Location map of study region. (a) Location of VA is highlighted as pink area and red box. (b) Black areas indicate two congressional districts, and red lines represent climate divisions in VA. (c) Location map of two congressional districts (VA06 and VA11). (d) Land use map of two districts. (e) Topography of two districts. Brown to yellow colors indicate lower elevations, while green to blue colors represent higher elevations. (For interpretation of the references to colour in this figure legend, the reader is referred to the web version of this article.)

Table 1
Land use characteristic for the two congressional districts.

Land use	VA06 (%)	VA11 (%)
Barren Land	0.1	0.4
Cultivated Crop	3.0	0.8
Developed Area	13	63.0
Forest	64.0	25.0
Grassland	0.3	0.3
Pasture/hay	19.9	0.4
Shrub	0.2	0.7
Water	0.6	5.6
Wetlands	0.0	3.8

RCP8.5 is an increasing radiative forcing pathway by 2100 (van Vuuren et al., 2011). Both RCP4.5 and RCP8.5 reflect diverse hydro-climatic conditions, and they have been used in numerous studies to evaluate the impacts of climate change on droughts (Kang and Sridhar, 2017; Kang and Sridhar, 2018; Jin et al., 2018).

For the VIC model simulation, three CMIP5 models are selected, BCC-CSM1.1, CanESM2, and CCSM4, to illustrate future (f1: 2017–2056, f2:2057–2096) hydrologic states. These models have been used to evaluate the climate change impacts on drought conditions in many river basins around the globe (Orlowsky and Seneviratne, 2013; Wang and Chen, 2014; Chattopadhyay et al., 2017; Kang and Sridhar, 2018).

2.4. Soil moisture and drought index

Soil moisture is an essential variable in the monitoring of crop growth and agricultural production by the United States Department of Agriculture (USDA) (Bolten et al., 2010). However, reliable estimation of regional soil moisture with limited ground observations is difficult due to spatial heterogeneity in soil properties, land cover, topography, and precipitation variability (Bolten et al., 2010). Model-based soil moisture estimation provides a practical alternative, and it is widely used for agricultural drought estimations and evaluations (Sridhar et al., 2006; Sheffield and Wood, 2008; Sridhar and Wedin, 2009; Sehgal et al., 2018). In this study, the VIC model is used to estimate the soil moisture as the basis for SSI calculation. For the computation of the SSI, the univariate form of the Gringorten plotting position formula (Eq. 1) (Gringorten, 1963) is used.

$$P(x_i) = \frac{i - 0.44}{n + 0.12} \quad (1)$$

where n is the number of observations, and i is the rank of the observed values from the smallest. The mean precipitation value is set to zero; values below zero indicate dry conditions, while values above zero indicate wet conditions. Table 3 shows the classification of SSI values, and lower values indicate higher drought severity.

3. Results and discussion

3.1. Historic and future climate

Fig. 4 shows the precipitation and temperature changes for each CMIP5 model for the two congressional districts (VA06 and VA11) for the historic and future periods. Fig. 4(a) and (b) present the results for the VA06 district, while Fig. 4(c) and (d) present the results for the VA11 district. The X-axis indicates the change in precipitation (%),

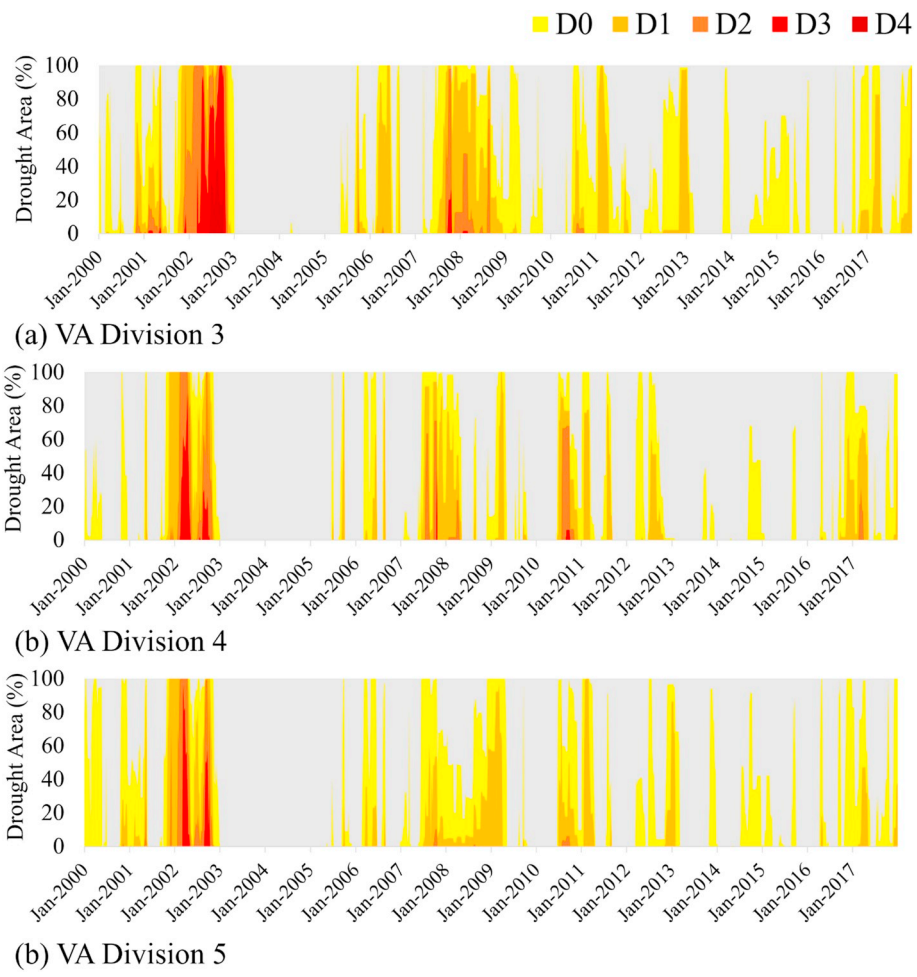

Fig. 3. Drought area maps for VA climate divisions from United States Drought Monitor (USDM) from January 2000 to December 2017. Each colour represents a different category of drought conditions. Yellow indicates the D0 category (Abnormal drought), orange indicates the D1 category (Moderate drought), darker orange indicates the D2 category (Severe drought), red indicates the D3 category (Extreme drought), and dark brown indicates the D4 category (Exceptional drought). (a) Drought area map for VA division 3. (b) Drought area map for VA division 4. (c) Drought area map for VA division 5. (For interpretation of the references to colour in this figure legend, the reader is referred to the web version of this article.)

Table 2
NAICS (North American Industry Classification System) classification for the agricultural sectors.

NAICS classification for Virginia	Sector description
1	Oilseed farming
2	Grain farming
3	Vegetable and melon farming
4	Fruit farming
7	Tobacco farming
10	All other crop farming
11	Beef cattle ranching and farming, including feedlots and dual-purpose ranching and farming
14	Animal production, except cattle and poultry and eggs

Table 3
Classification of the Standardized Soil moisture Index (SSI) (McKee et al., 1993).

SSI Values	Drought category
2.0 and above	Extremely Wet
1.50–1.99	Very Wet
1.00–1.49	Moderately Wet
−0.99–0.99	Near normal
−1.00 - -1.49	Moderate Drought
−1.50 - -1.99	Severe Drought
−2.0 or less	Extreme Drought

while the Y-axis shows the change in temperature (°C). Also, the blue dots indicate the results of RCP4.5, and the red dots indicate the results of RCP8.5. Since the concepts of the two pathways are different (van Vuuren et al., 2011), there are considerable variations of precipitation and temperature between the two RCPs.

For the VA06 district and f1 period, the maximum precipitation increase is 7.3% for the CCSM4-RCP4.5, and the maximum temperature increase is 2.6 °C for the CanESM2-RCP8.5 model. In contrast, there is a 4.2% decrease in precipitation for the CanESM2-RCP4.5 model and f1 period, and the minimum temperature increase is 1.9 °C for the BCC-CSM1.1-RCP4.5 model. For the f2 period, the maximum precipitation increase is 14.8% for the CCSM4-RCP8.5 model, and the maximum temperature increase is 5.2 °C for the CCSM4-RCP4.5 model. In contrast, there is 0.3% decrease in precipitation for the BCC-CSM1.1-RCP4.5 model, and the minimum temperature increase is 2.8 °C for the CCSM4-RCP4.5 model.

For the VA11 district and f1 period, the maximum precipitation increase is 10.9% for the CCSM4-RCP4.5, and the maximum temperature increase is 2.5 °C for the CanESM2-RCP8.5 model. In contrast, there is a 4.6% decrease in precipitation for the CanESM2-RCP4.5 model, and the minimum temperature increase is 1.7 °C for the BCC-CSM1.1-RCP4.5 model. For the f2 period, the maximum precipitation increase is 15.7% for the CCSM4-RCP8.5 model, and the maximum temperature increase is 5.2 °C for the CanESM2-RCP8.5 model. In contrast, there is 0.1% decrease in precipitation for the CanESM2-RCP4.5 model, and the minimum temperature increase is 2.5 °C for the CCSM4-RCP4.5 model. Overall, two districts have analogous patterns of

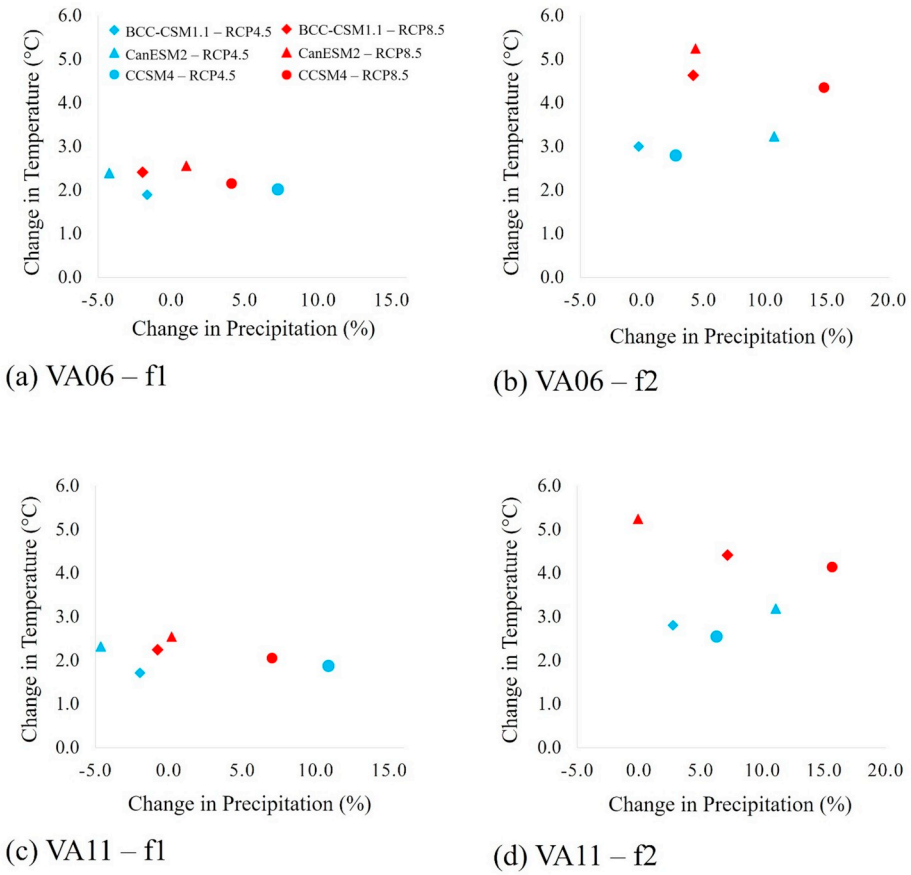

Fig. 4. Scatter plots of change in precipitation and temperature for the CMIP5 climate models of each district. X-axis is the change in precipitation (%), and Y-axis is the change in temperature (°C). Different markers represent the results of each climate model. Blue markers indicate the results of RCP4.5, and red markers indicate the results of RCP8.5. (a) Results of VA06 - f1 period (2017–2056). (b) Results of VA06 – f2 period (2057–2096). (c) Results of VA11 - f1 period (2017–2056). (d) Results of VA11 – f2 period (2057–2096). (For interpretation of the references to colour in this figure legend, the reader is referred to the web version of this article.)

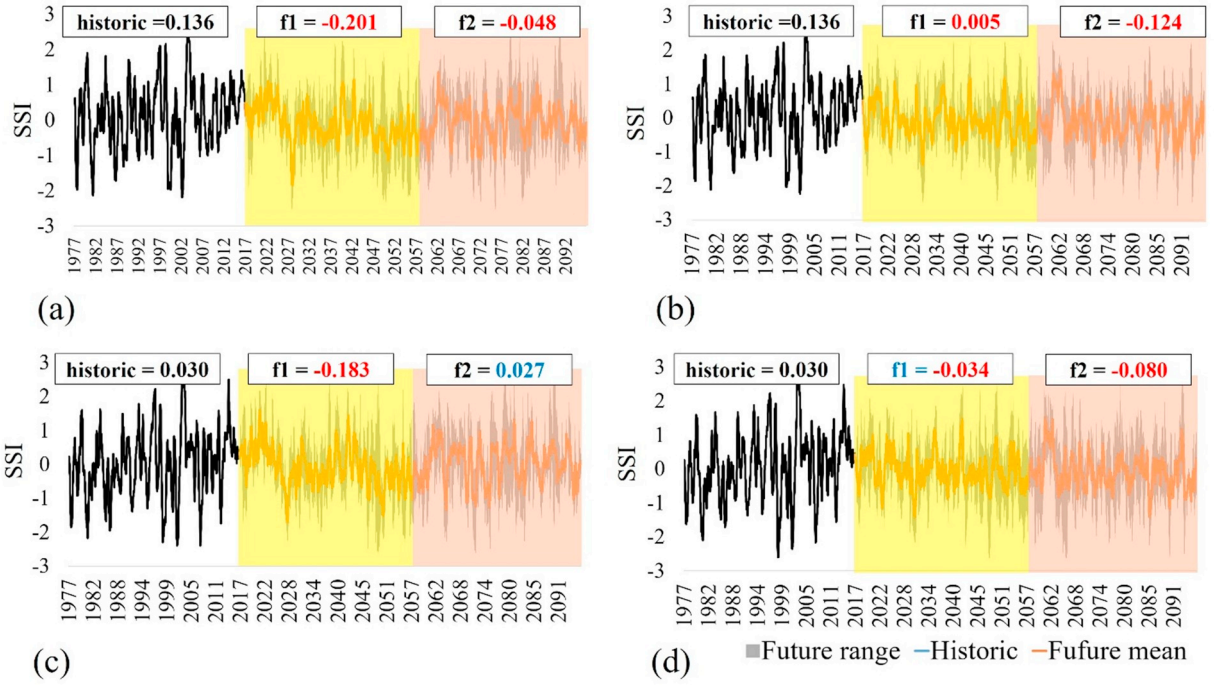

Fig. 5. Weekly time series of SSI for each congressional district. The black lines indicate the mean values for the historic period, and the orange lines are the mean values for the future periods from the three climate models. The gray areas indicate the range of climate models for the future periods. The transparent yellow and orange rectangles highlight the future periods. For all figures, red text indicates an increase in drought severity, while blue text indicates a decrease in drought severity in the future. (a) Results of VA06 for RCP4.5. (b) Results of VA06 for RCP8.5. (c) Results of VA11 for RCP4.5. (d) Results of VA11 for RCP8.5. (For interpretation of the references to colour in this figure legend, the reader is referred to the web version of this article.)

Table 4
Mean values of the SSI for the historic and future periods of each climate model. Red text means an increase in drought severity, while blue text represents a decrease in drought severity in the future.

District	RCPs	Climate models	historic	f1 (mean)	f2 (mean)	f1	f2
All districts	RCP4.5	BCC-CSM1.1	0.116	−0.077	−0.041	−0.080	−0.183
		CanESM2				−0.384	0.220
		CCSM4				0.157	−0.201
	RCP8.5	BCC-CSM1.1		−0.067	−0.085	−0.137	−0.172
		CanESM2				−0.027	−0.288
		CCSM4				−0.105	0.122
VA06	RCP4.5	BCC-CSM1.1	0.136	−0.104	−0.058	−0.080	−0.188
		CanESM2				−0.385	0.221
		CCSM4				0.155	−0.208
	RCP8.5	BCC-CSM1.1		−0.092	−0.114	−0.139	−0.178
		CanESM2				−0.029	−0.285
		CCSM4				−0.109	0.121
VA11	RCP4.5	BCC-CSM1.1	0.030	−0.183	0.027	−0.085	−0.075
		CanESM2				−0.358	0.194
		CCSM4				0.201	−0.062
	RCP8.5	BCC-CSM1.1		−0.034	−0.080	−0.106	−0.039
		CanESM2				0.007	−0.347
		CCSM4				−0.002	0.145

climates except for the precipitation changes from CanESM2. Since each climate model has various background and developed by different institutes, they have different precipitation and temperature patterns in the future periods. These variabilities enable an analysis of the range of diverse influences of climate change on droughts and agricultural productions.

3.2. Time series of SSI and drought occurrences for districts

Fig. 5 shows the weekly time series of SSI for the two RCP models (4.5 and 8.5) and two districts, and Table 4 presents the mean SSI values for each congressional district. As shown in Table 3, lower values of SSI indicate drought conditions, while higher values represent wet conditions. In general, future drought severity, estimated by SSI, increases for the study area. However, considerable variations in projections are found across the districts. In Fig. 5, an increase in drought severity is highlighted with red text, while a decrease in drought severity is highlighted with blue text.

For the results of VA06, the mean values for future periods of RCP4.5 are −0.104 (f1) and − 0.058 (f2), and those of RCP8.5 are −0.092 (f1) and −0.114 (f2), which indicate an increase in drought severity in the future. However, some climate models and periods such as CanESM2 – RCP4.5 for the f2 period and CCSM – RCP4.5 for the f1 period indicate a decrease in drought severity in the future. The CanESM2 – RCP4.5 for the f2 period and CanESM2 – RCP4.5 for the f1 period show the highest precipitation increase among the climate models of RCP4.5 (Fig. 4(a) and (b)). These periods influence the decreases in drought severity. Besides, the highest precipitation increase is estimated by the CCSM - RCP8.5 for the f2 period among the climate models of RCP8.5, and the drought severity is relatively similar to the historic period since a scale of temperature increase is higher than the models of RCP4.5.

For the results of VA11, the mean values for future periods of RCP4.5 are −0.183 (f1) and 0.027 (f2), and those of RCP8.5 are −0.034 (f1) and −0.080 (f2), which indicate an overall increase in drought severity in the future. Similar to VA06, there are decreases in drought severity for the results of CanESM2 – RCP4.5 for the f2 period, CanESM2 – RCP4.5 for the f1 period, and CCSM - RCP8.5 for the f2 period, which show higher precipitation increases in the future periods.

Fig. 6 shows the seasonal comparisons of the mean soil moisture values (total column moisture). Solid black lines represent the weekly mean values of the historic period (1977–2016), and gray areas indicate the range of future periods and RCPs. Fig. 6(a) and (b) represent the results of the VA06 district in f1 and f2 periods, respectively. There is projected overall decrease in soil moisture during the period of early April to late February, which includes the crop-growing season (April to September). The VA06 district primarily consists of forest (67%), and an increase in temperature in this region leads to an evapotranspiration increase that decreases the amount of soil moisture. These increased in evapotranspiration for VA06 are highlighted in Fig. 7(a) and (b) for the f1 and f2 periods, respectively. By contrast, Fig. 6(c) and (d) show the results of the VA11 district where less notable trends in soil moisture. The VA11 district is mainly composed of developed areas (63%) and includes some forest regions (25%). Thus, the temperature increase in the VA11 district does not increase evapotranspiration as much as it does in the VA06 district (Fig. 7(c) and (d)), and the precipitation increase in the future translate into an increase in soil moisture.

In the VA06 district, the lowest SSI values are −0.385 for the f1 period of CanESM2-RCP4.5 model, and −0.285 for the f2 period and CanESM2-RCP8.5 model. In Fig. 5(a) and (b), the CanESM2-RCP4.5 model is the driest in the f1 period (blue triangle), and the CanESM2-RCP8.5 model is the hottest in the f2 period (red triangle). In the VA11 district, the lowest SSI values are −0.358 for the f1 period of CanESM2-RCP4.5 model, and −0.347 for the f2 period and CanESM2-RCP8.5 model. In Fig. 5(c) and (d), the CanESM2-RCP4.5 model is the driest in the f1 period (blue triangle), and the CanESM2-RCP8.5 model is the driest and hottest in the f2 period (red triangle). Thus, these results imply that a decrease in precipitation and an increase in temperature are the primary drivers of the increase in green water droughts in future periods. Table 5 and Table 6 show the annual mean soil moisture and ET for the historic and future periods, and their percentage differences. Generally, the magnitude of soil moisture and ET differences for VA06 are higher than for VA11, and it is due to the different land use compositions.

Fig. 8 presents the spatial maps of the drought occurrence ratios based on the SSI results for the study areas. The maps of the drought occurrence odds ratios are computed based on the division of numbers of historic and future drought occurrences for each grid (future/historic). A value corresponding to or greater than one is shown in orange or red and demonstrates an increase in drought occurrence in the future period, while values less than one are shown in yellowish green and dark green and demonstrate a decrease in drought occurrences in the future. Additionally, the mean values of drought occurrence ratios are marked in each figure. For the VA06 and VA11 districts, there are general increases in drought occurrences for the BCC-CSM1.1 and CanESM2 models, while there is a decrease in the CCSM4 model. Again, the overall magnitude of drought occurrence for VA06 is greater than VA11.

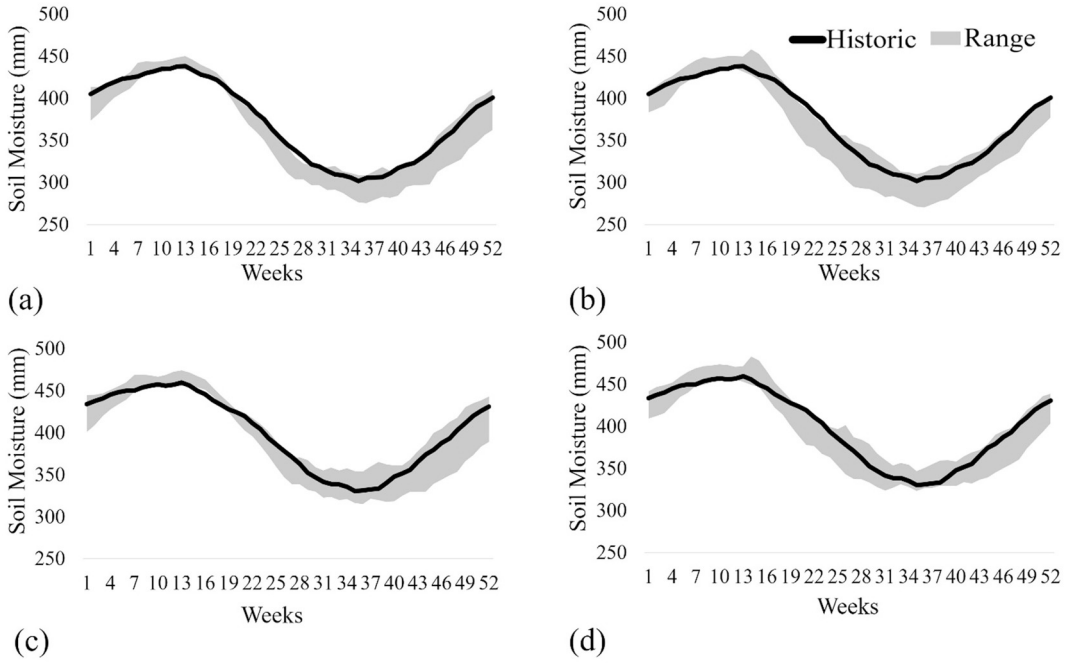

Fig. 6. Seasonal comparisons of mean soil moisture values for each congressional district. The X-axis represents the weeks of the year, and the Y-axis represents the weekly mean soil moisture values (total column, mm). (a) Results of VA06 for RCP4.5. (b) Results of VA06 for RCP8.5. (c) Results of VA11 for RCP4.5. (d) Results of VA11 for RCP8.5.

Similar to the time series, the drought occurrences results are strongly influenced by precipitation and temperature change projections. For example, the CCSM4 model shows the highest increase in precipitation except for the RCP4.5 and f2 period (blue circle in Fig. 4(b)), and it results in the decrease of drought occurrences. In contrast, there are increases in drought occurrences from the other two models (BCC-CSM1.1 and CanESM2) because the magnitude of the precipitation increase is lower than in the CCSM4 model. The highest drought occurrence ratio of 2.95, from the CanESM2-RCP8.5 model in the f2 period, is due to a high temperature increase but a relatively low precipitation increase.

3.3. Regression analysis of output and annual mean SSI values

Simple linear regression analysis is carried out to identify the relationships between the annual mean SSI values and value of primarily

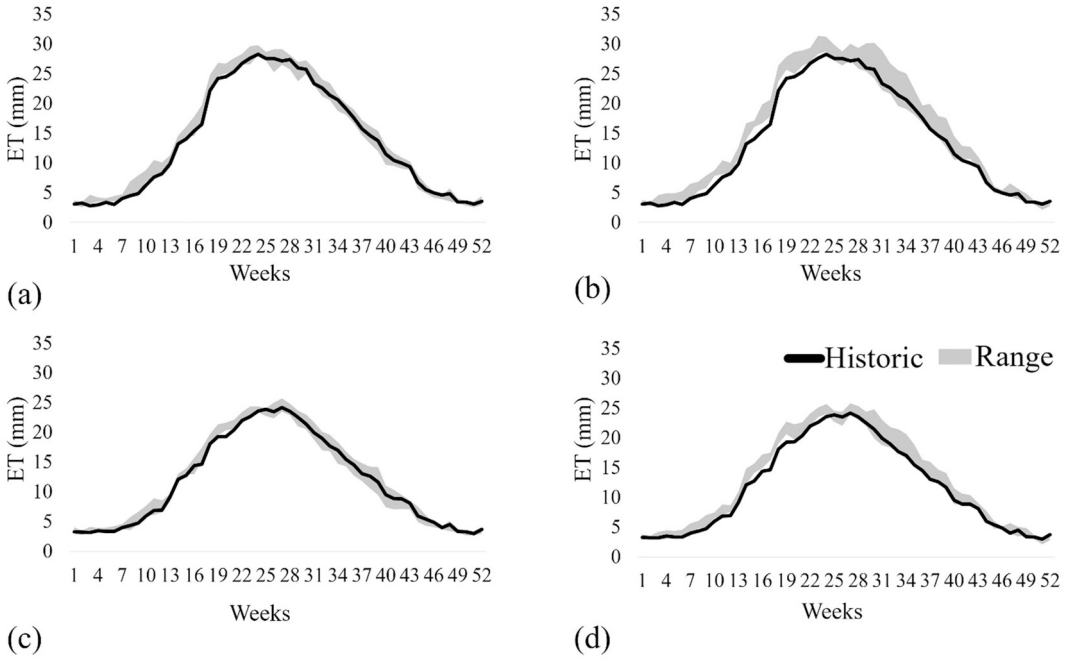

Fig. 7. Seasonal comparisons of the mean values of evapotranspiration (ET) for each congressional district. The X-axis represents the weeks of the year, and the Y-axis represents the weekly mean values of ET (mm). (a) Results of VA06 for RCP4.5. (b) Results of VA06 for RCP8.5. (c) Results of VA11 for RCP4.5. (d) Results of VA11 for RCP8.5.

Table 5
Mean values of the soil moisture for the historic and future periods of each climate model.

District	Historic annual soil moisture (mm)	RCPs	Climate models	f1 period	f2 period	Percentage Change (f1)	Percentage Change (f2)	Mean (f1)	Mean (f2)
VA06	372.9	RCP4.5	BCC-CSM1.1	362.0	359.0	−2.9	−3.7	−2.3	−2.0
			CanESM2	354.5	375.7	−4.9	0.8		
			CCSM4	376.5	366.0	1.0	−1.9		
		RCP8.5	BCC-CSM1.1	360.0	359.3	−3.5	−3.7		
			CanESM2	361.4	354.7	−3.1	−4.9		
			CCSM4	370.8	377.1	−0.6	1.1		
VA11	400.4	RCP4.5	BCC-CSM1.1	393.2	394.9	−1.8	−1.4	−0.9	−0.6
			CanESM2	384.2	402.4	−4.0	0.5		
			CCSM4	411.4	403.4	2.8	0.7		
		RCP8.5	BCC-CSM1.1	395.2	398.0	−1.3	−0.6		
			CanESM2	391.1	381.3	−2.3	−4.8		
			CCSM4	405.0	408.2	1.2	2.0		

Table 6
Mean values of the ET for the historic and future periods of each climate model.

District	historic annual ET (mm)	RCPs	Climate models	f1 period	f2 period	Percentage Change (f1)	Percentage Change (f2)	Mean (f1)	Mean (f2)
VA06	713.7	RCP4.5	BCC-CSM1.1	728.3	734.1	2.0	2.9	3.4	9.1
			CanESM2	716.7	786.6	0.4	10.2		
			CCSM4	766.7	748.9	7.4	4.9		
		RCP8.5	BCC-CSM1.1	733.2	766.9	2.7	7.4		
			CanESM2	729.1	807.2	2.2	13.1		
			CCSM4	754.8	828.2	5.8	16.0		
VA11	614.8	RCP4.5	BCC-CSM1.1	616.3	629.8	0.2	2.4	2.1	7.3
			CanESM2	605.5	662.9	−1.5	7.8		
			CCSM4	654.7	646.6	6.5	5.2		
		RCP8.5	BCC-CSM1.1	622.1	657.5	1.2	6.9		
			CanESM2	615.9	662.6	0.2	7.8		
			CCSM4	650.9	697.4	5.9	13.4		

rain-fed agricultural output in the two Virginia congressional districts. The studentized residual method is used to identify and exclude outliers. Fig. 9 shows the results of the analysis, where the X-axis represents the annual means of SSI and the Y-axis represents the annual agricultural production for seven years (2010–2016). Specifically, the Y-axis of Fig. 9 represents the sum of the annual agricultural products described in Table 2 that are primarily affected by rain-fed productions, but partially mixed with irrigated productions. The selected sectors account for 18% (VA06) and 39% (VA11) of total agricultural production in 2016, respectively.

The results for all districts show a strong linear relationship between the annual mean SSI values and the sum of agricultural production. For the VA06 district results, the adjusted R^2 is 0.78. The SSI parameter estimate of interest is 1.36×10^8, which is statistically significant at the $p = .05$ level. The highest mean SSI value and the sum of agricultural production are 1.00 and $379,000,000, respectively, in 2016, when the highest precipitation occurs in the VA06 district (1139 mm). The lowest SSI and the sum of agricultural production are 0.15 and $263,000,000, respectively, in 2010, when the second-lowest level of precipitation occurs (963 mm). For the VA11 district, the adjusted R^2 are 0.88. The SSI parameter estimate of interest is 3.28×10^5, which is statistically significant at the p = .05 level. The highest mean SSI value and the sum of agricultural production are 1.37 and $1,370,000, respectively, in 2016, when the highest precipitation occurs in the VA11 district (1304 mm). However, the lowest SSI and the sum of agricultural production are −0.08 and $840,000, respectively, in 2010, when the lowest precipitation occurs (1031 mm). Since the SSI regression parameter estimates are significant, it is reasonable to apply the agricultural response of SSI parameter estimates to the impact of drought on agricultural production.

3.4. Climate change impacts on agricultural productions

Table 7 shows the mean values of agricultural production for both historic (1977–2016) and future periods based on the estimated relationships between SSI levels and agricultural productions. In Table 7, increases in agricultural production are highlighted with blue, while decreases are highlighted with red. For the VA06 district, future climate change projection results in overall decreases in agricultural production. The mean value of agricultural production for the historic period is $277,000,000/year. Agricultural production is projected to decrease in future periods by 11.6% in the f1 period for the RCP4.5 model and by 11.2% for the RCP8.5 model. Similarly, mean decreases of 9.4% and 15.9% are found in the f2 period for the RCP4.5 and RCP8.5 models, respectively. However, significant variability remains in future production predictions. The highest production prediction for the future period is a 4.3% increase in the CanESM2-RCP8.5 model for the f2 period, while the lowest production prediction is a 25.3% decrease in the CanESM2-RCP4.5 model for the f1 period.

For the VA11 district, the mean value of agricultural production for the historic period is $876,000/year. Agricultural production decreases of 4.1% and 2.4% for the f1 period and 0.5% and 4.1% for the f2 period under the RCP4.5 and RCP8.5 models, respectively. Again, there is significant variability in future predictions, ranging from a 6.4% increase in the CCSM4-RCP4.5 model for the f1 period, to a 14.5% decrease in the CanESM2-RCP4.5 model for the f1 period.

3.5. Assessment of economy-wide impacts using IMPLAN

We now estimate the economy-wide gains or losses associated with future climate change. Table 8 shows the results of economy-wide impacts using the IMPLAN model based on the mean values of the various climate models. Direct effects, indirect effects, and induced effects are examined for employment (number of jobs), labor income ($), and output ($). The direct effects are economic losses or gains in the agricultural sector, the indirect effects are economic losses or gains in associated sectors supplying the agricultural sector, induced effects are changes in economic activity arising from changing overall economic

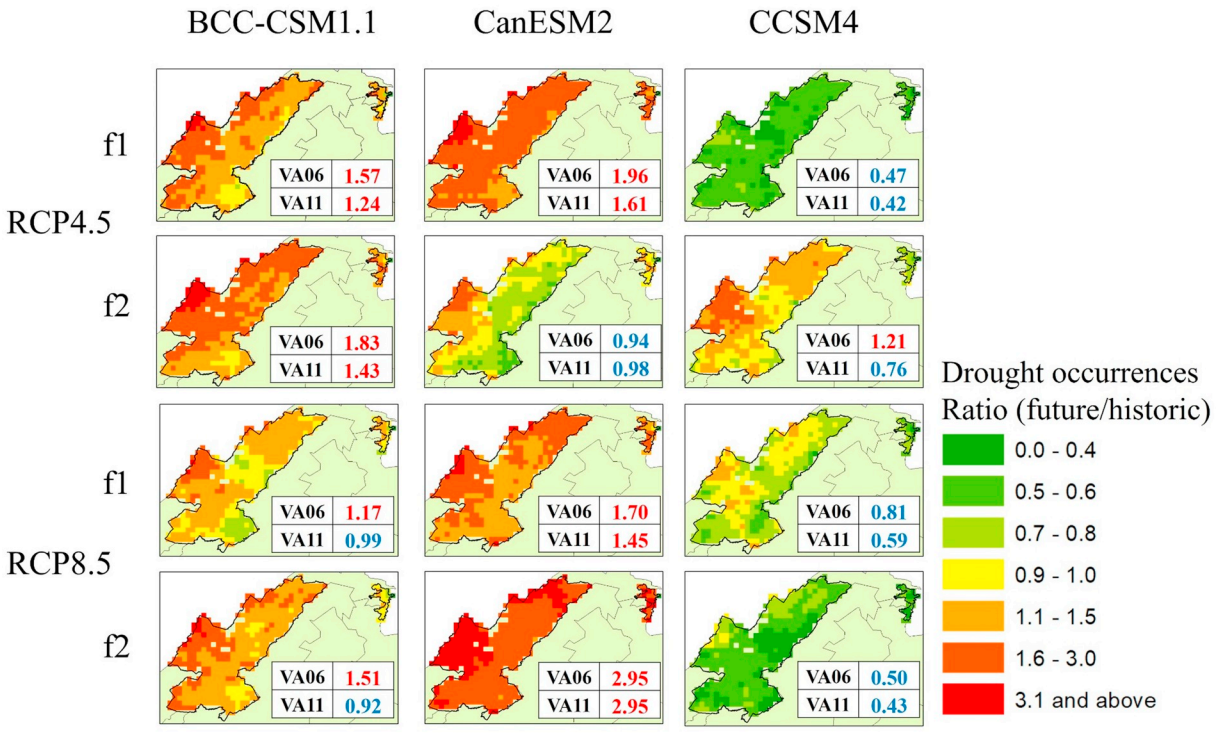

Fig. 8. Spatial maps of drought occurrences based on results of SSI between historic and future periods. A value equal to or > 1 indicates an increase in drought occurrences in the future and is symbolized as orange to red, while a value < 1 is represented as yellow to green and indicates a decrease in drought occurrences in the future. Inside the figure, red text represents an increase in drought occurrence, while blue text represents a decrease in drought occurrence in the future. (For interpretation of the references to colour in this figure legend, the reader is referred to the web version of this article.)

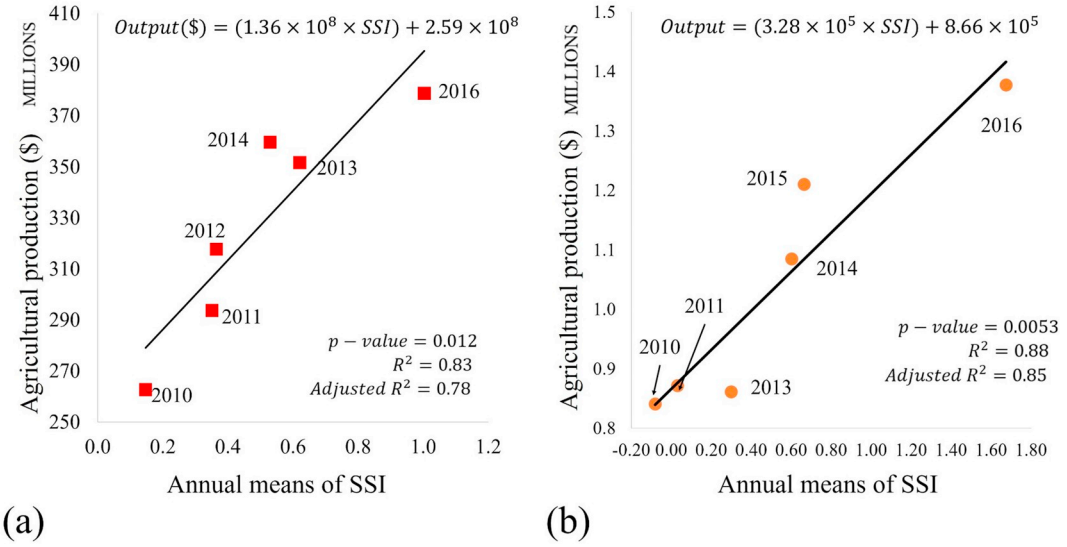

Fig. 9. Scatter plots showing correlations between annual means of SSI and sum of agricultural production ($) for seven years (2010–2016). The X-axis represents the annual mean SSI values, and the Y-axis is the sum of agricultural production ($). (a) Results of VA06. (b) Results of VA11.

activity (e.g., decreased consumption and increased unemployment) driven by spillovers across the economy, and total effects are the sum of the direct, indirect, and induced effects. Future agricultural sector impacts may be lower due to farmer's adaptions. But Burke and Emerick (2016) find that long-term adaptation has likely mitigated more of the short-term agricultural impacts of extreme events.

Climate change influences on green water droughts are estimated to decrease the number of agricultural sector jobs in the VA06 district by 12.9% to 16.7% (total effect) compared to 2016 through direct, indirect, and induced effects on agricultural production changes (Table 8). In addition, agricultural sector output (total agricultural value added) decreases by 16.8% to 21.7% compared to 2016. The number of agricultural jobs in the less agriculturally intensive VA11 district decreases by 0.4% to 4.3% (total effect), and the agricultural sector value added decreases by 0.5% to 5.1% compared to 2016. Table 9 presents the size of total economy in the two districts and proportions of the selected sectors, and the two districts are relatively small: 0.3170% and 0.0010% for total value added in the VA06 and VA11 districts, respectively.

Finally, Table 10 shows the impacts of green water droughts on total

Table 7
Mean values of sum of agricultural production for historic and future periods for each climate model (unit: million $/year). Bold text represents a decrease in agricultural production, while italicized text represents an increase in agricultural production.

District	RCPs	Climate models	Historic	f1 (mean)	f2 (mean)	f1	f2
			(Million $)	(Unit: %)	(Unit: %)	(Unit: %)	(Unit: %)
VA06	RCP4.5	BCC-CSM1.1	277	**-11.6**	**-9.4**	**-10.5**	**-15.9**
		CanESM2				**-25.3**	*4.3*
		CCSM4				*1.1*	-16.6
	RCP8.5	BCC-CSM1.1		**-11.2**	**-15.9**	**-13.4**	**-15.2**
		CanESM2				**-7.9**	**-20.6**
		CCSM4				**-11.9**	**-0.7**
VA11	RCP4.5	BCC-CSM1.1	0.876	**-4.1**	*0.5*	**-4.3**	**-4.0**
		CanESM2				**-14.5**	*6.2*
		CCSM4				*6.4*	**-3.4**
	RCP8.5	BCC-CSM1.1		**-2.4**	**-4.1**	**-5.1**	**-2.6**
		CanESM2				**-0.9**	**-14.2**
		CCSM4				**-1.3**	*4.2*

Table 8
Mean values of economy-wide impacts on future agricultural sector.

historic	RCPs	Periods	Impact type	Employment (%)	Labor income (%)	Output (%)
VA06	RCP4.5	f1	Direct Effect	−11.6	−11.4	−11.5
			Indirect Effect	−3.1	−5.8	−5.5
			Induced Effect	−1.2	−3.9	−3.7
			Total Effect	**−15.9**	**−21.2**	**−20.7**
		f2	Direct Effect	−9.4	−9.3	−9.3
			Indirect Effect	−2.5	−4.7	−4.5
			Induced Effect	−1.0	−3.2	−3.0
			Total Effect	**−12.9**	**−17.2**	**−16.8**
	RCP8.5	f1	Direct Effect	−11.1	−10.9	−11.0
			Indirect Effect	−3.0	−5.6	−5.3
			Induced Effect	−1.2	−3.8	−3.6
			Total Effect	**−15.2**	**−20.3**	**−19.8**
		f2	Direct Effect	−12.2	−12.0	−12.1
			Indirect Effect	−3.3	−6.1	−5.8
			Induced Effect	−1.3	−4.1	−3.9
			Total Effect	**−16.7**	**−22.3**	**−21.7**
VA11	RCP4.5	f1	Direct Effect	−4.2	−4.1	−4.1
			Indirect Effect	0.0	−2.3	−0.6
			Induced Effect	0.0	−1.2	−0.3
			Total Effect	**−4.2**	**−7.6**	**−5.1**
		f2	Direct Effect	−0.4	−0.4	−0.4
			Indirect Effect	0.0	−0.2	−0.1
			Induced Effect	0.0	−0.1	0.0
			Total Effect	**−0.4**	**−0.8**	**−0.5**
	RCP8.5	f1	Direct Effect	−2.4	−2.4	−2.4
			Indirect Effect	0.0	−1.3	−0.4
			Induced Effect	0.0	−0.7	−0.2
			Total Effect	**−2.5**	**−4.5**	**−3.0**
		f2	Direct Effect	−4.2	−4.1	−4.2
			Indirect Effect	0.0	−2.3	−0.6
			Induced Effect	0.0	−1.3	−0.3
			Total Effect	**−4.3**	**−7.7**	**−5.1**

Table 9
Total industry outputs and proportions of selected agricultural sectors in 2016.

	Total industry output ($)	Employment (%)	Income (%)	Industry output (%)
VA06	65,184,166,740	1.1957	0.3016	0.3170
VA11	86,283,111,683	0.0115	0.0002	0.0010

economy of the two districts. The shares of agriculture in total production in the districts drive the results. The direct, indirect, and induced effects of agriculture (i.e., green water effects) on total economy in the districts drive the results. There is an overall decrease in the economic outputs of about 0.05–0.07% in the VA06 district and the 'Direct Effect' mainly causes them. In addition, there is virtually no change (a 0.0001% decrease in total) in the VA11 district. Thus, the strong impacts of climate change on the agricultural sectors have very limited broader economy-wide impacts in these economically diverse congressional districts.

4. Conclusion

The impacts of climate change on agricultural droughts and production are important determinants of the societal costs of climate change. This paper focuses on the economic losses associated with changes in drought severity. Long-term economic impacts in two congressional districts in Northern VA are estimated using the soil moisture simulation from the VIC model and SSI based on climate projection models from CMIP5 models. Simulations of future soil moisture and agricultural droughts using SSI indicate that climate change will lead to

Table 10
Mean values of impacts of green water droughts on total economy.

historic	RCPs	Periods	Impact type	Employment (%)	Labor income (%)	Output (%)
VA06	RCP4.5	f1	Direct Effect	−0.1381	−0.0344	−0.0364
			Indirect Effect	−0.0372	−0.0176	−0.0174
			Induced Effect	−0.0146	−0.0119	−0.0118
			Total Effect	**−0.1900**	**−0.0639**	**−0.0655**
		f2	Direct Effect	−0.1122	−0.0280	−0.0296
			Indirect Effect	−0.0302	−0.0143	−0.0141
			Induced Effect	−0.0119	−0.0096	−0.0096
			Total Effect	−0.1543	−0.0519	−0.0532
	RCP8.5	f1	Direct Effect	−0.1324	−0.0330	−0.0349
			Indirect Effect	−0.0356	−0.0169	−0.0167
			Induced Effect	−0.0140	−0.0114	−0.0113
			Total Effect	**−0.1820**	**−0.0612**	**−0.0628**
		f2	Direct Effect	−0.1453	−0.0362	−0.0383
			Indirect Effect	−0.0391	−0.0185	−0.0183
			Induced Effect	−0.0154	−0.0125	−0.0124
			Total Effect	**−0.1998**	**−0.0672**	**−0.0689**
VA11	RCP4.5	f1	Direct Effect	−0.0005	0.0000	−0.00004
			Indirect Effect	0.0000	0.0000	−0.00001
			Induced Effect	0.0000	0.0000	0.00000
			Total Effect	**−0.0005**	**0.0000**	**−0.00005**
		f2	Direct Effect	0.0000	0.0000	0.0000
			Indirect Effect	0.0000	0.0000	0.0000
			Induced Effect	0.0000	0.0000	0.0000
			Total Effect	**0.0000**	**0.0000**	**0.0000**
	RCP8.5	f1	Direct Effect	−0.0003	0.0000	0.0000
			Indirect Effect	0.0000	0.0000	0.0000
			Induced Effect	0.0000	0.0000	0.0000
			Total Effect	**−0.0003**	**0.0000**	**0.0000**
		f2	Direct Effect	−0.0005	0.0000	0.0000
			Indirect Effect	0.0000	0.0000	0.0000
			Induced Effect	0.0000	0.0000	0.0000
			Total Effect	**−0.0005**	**0.0000**	**−0.0001**

an overall increase in drought occurrences with the mean values of drought occurrences 1.38 and 1.15 times higher across all future climate models compared to the historic period in the VA06 and VA11 districts, respectively.

Drought impacts differ in the two districts due to differences in land use influences on water budget components, such as ET and soil moisture, of the hydrological model. This analysis also suggests that increased incidence of green water droughts directly translate into decreases in agricultural production (Tables 4 and 7). However, land use and associated economic sector composition of districts generate different aggregate economic impacts. Thus, geographic (e.g., land-use) and economic structures need to be incorporated for accurate estimation of the societal costs of climate change. Further, climate change pathways are likely to differ in rural and urban settings. Additional research is needed to future identify and quantify the alternative impact pathways in rural and urban areas with a consideration of blue water availability and flexibility (e.g., reservoir operation, groundwater pumping), which play significant roles to determine the economic impact of droughts.

Acknowledgement

This project was funded, in part, by the Virginia Agricultural Experiment Station (Blacksburg) and the Hatch Program of the National Institute of Food and Agriculture, U.S Department of Agriculture (Washington, D.C.). We also thank Institute for Critical Technology and Applied Science (ICTAS), Graduate School at Virginia Tech for the graduate fellowship provided to the first author during his graduate education.

References

Abatzoglou, J.T., 2013. Development of gridded surface meteorological data for ecological applications and modelling. Int. J. Climatol. 33 (1), 121–131.

Bauman, A., Goemans, C., Pritchett, J., McFadden, D.T., 2013. Estimating the economic and social impacts from the drought in Southern Colorado. J. Contemp. Water Res. Educ. 151 (1), 61–69.

Bolten, J.D., Crow, W.T., Zhan, X., Jackson, T.J., Reynolds, C.A., 2010. Evaluating the utility of remotely sensed soil moisture retrievals for operational agricultural drought monitoring. IEEE J. Sel. Top. Appl. Earth Observations Remote Sen. 3 (1), 57–66.

Burke, M., Emerick, K., 2016. Adaptation to climate change: evidence from US agriculture. Am. Econ. J. Econ. Pol. 8 (3), 106–140.

Calatrava, J., Garrido, A., 2005. Spot water markets and risk in water supply. Agric. Econ. 33 (2), 131–143.

Cayan, D.R., Das, T., Pierce, D.W., Barnett, T.P., Tyree, M., Gershunov, A., 2010. Future dryness in the southwest US and the hydrology of the early 21st century drought. Proc. Natl. Acad. Sci. 107 (50), 21271–21276.

Chattopadhyay, S., Edwards, D.R., Yu, Y., Hamidisepehr, A., 2017. An assessment of climate change impacts on future water availability and droughts in the Kentucky River Basin. Environ. Processes 4 (3), 477–507.

Cheng, L., Hoerling, M., AghaKouchak, A., Livneh, B., Quan, X.W., Eischeid, J., 2016. How has human-induced climate change affected California drought risk? J. Clim. 29 (1), 111–120.

CHJ, 2007. Plan especial de alerta y eventual sequía en la Confederación Hidrográfica del Jucar Confederación Hidrográfica del Júcar, Valencia, España. Retrieved from www.chj.es. Last access December 2016 (in Spanish).

Combs, S., 2012. The Impact of the 2011 Drought and Beyond. Texas Comptroller of Public Accounts, Austin, TX, USA.

Dai, A., 2011. Drought under global warming: a review. Wiley Interdiscip. Rev. Clim. Chang. 2 (1), 45–65.

Ding, Y., Hayes, M.J., Widhalm, M., 2011. Measuring economic impacts of drought: a review and discussion. Disaster Prevent. Manage. Int. J. 20 (4), 434–446.

Drought Response Technical Advisory Committee (DRTAC), 2003. Virginia Drought Assessment and Response Plan.

Faust, A.K., Gonseth, C., Vielle, M., 2015. The economic impact of climate-driven changes in water availability in Switzerland. Water Policy 17 (5), 848–864.

Freire-González, J., Decker, C.A., Hall, J.W., 2017a. A scenario-based framework for assessing the economic impacts of potential droughts. Water Econ. Policy 3 (4), 1750007.

Freire-González, J., Decker, C., Hall, J.W., 2017b. The economic impacts of droughts: a framework for analysis. Ecol. Econ. 132, 196–204.

Gil Sevilla, M., Garrido Colmenero, A., Hernández-Mora Zapata, N., 2013. Direct and indirect economic impacts of drought in the agri-food sector in the Ebro River basin (Spain). Nat. Hazards Earth Syst. Sci. 3, 2679–2694.

Guerrero, B., 2012. The Impact of Agricultural Drought Losses on the Texas Economy, 2011. Briefing Paper. AgriLife Extension.

Hoekema, D.J., Sridhar, V., 2013. A system dynamics model for conjunctive management of water resources in the Snake River basin. J. Am. Water Resour. Assoc. 49 (6),

1327–1350. https://doi.org/10.1111/jawr.12092.
Howitt, R., Medellín-Azuara, J., MacEwan, D., Lund, J.R., Sumner, D., 2014. Economic Analysis of the 2014 Drought for California Agriculture. University of California, Davis, CA: Center for Watershed Sciences.
Howitt, R., Medellín-Azuara, J., MacEwan, D., Lund, J.R., Sumner, D., 2015. Economic analysis of the 2015 Drought for California Agriculture. University of California, Davis, CA: Center for Watershed Sciences.
Intergovernmental Panel on Climate Change (IPCC), 2014. In: Core Writing Team, Pachauri, R.K., Meyer, L.A. (Eds.), Climate Change 2014: Synthesis Report. Contribution of Working Groups I, II and III to the Fifth Assessment Report of the Intergovernmental Panel on Climate Change. IPCC, Geneva, Switzerland, pp. 151.
Jin, Z., Ainsworth, E.A., Leakey, A.D., Lobell, D.B., 2018 Feb. Increasing drought and diminishing benefits of elevated carbon dioxide for soybean yields across the US Midwest. Glob. Chang. Biol. 24 (2), e522–e533.
Kang, H., Sridhar, V., 2017. Combined statistical and spatially distributed hydrological model for evaluating future drought indices in Virginia. J. Hydrol. 12, 253–272.
Kang, H., Sridhar, V., 2018. Assessment of future drought conditions in the chesapeake bay watershed. J. Am. Water Resour. Assoc. 54 (1), 160–183. https://doi.org/10.1111/1752-1688.12600.
Karl, T.R., Gleason, B.E., Menne, M.J., McMahon, J.R., Heim Jr., R.R., Brewer, M.J., Kunkel, K.E., Arndt, D.S., Privette, J.L., Bates, J.J., Groisman, P.Y., 2012. US temperature and drought: Recent anomalies and trends. EOS Trans. Am. Geophys. Union 93 (47), 473–474.
Leng, G., Tang, Q., Rayburg, S., 2015. Climate change impacts on meteorological, agricultural and hydrological droughts in China. Glob. Planet. Chang. 126, 23–34.
Liang, X., Lettenmaier, D.P., Wood, E.F., Burges, S.J., 1994. A simple hydrologically based model of land surface water and energy fluxes for general circulation models. J. Geophys. Res. Atmos. 99 (D7), 14415–14428.
Livneh, B., Rosenberg, E.A., Lin, C., Nijssen, B., Mishra, V., Andreadis, K.M., Maurer, E.P., Lettenmaier, D.P., 2013. A long-term hydrologically based dataset of land surface fluxes and states for the conterminous United States: update and extensions. J. Clim. 26.
Logar, I., van den Bergh, J.C., 2013. Methods to assess costs of drought damages and policies for drought mitigation and adaptation: review and recommendations. Water Resour. Manag. 27 (6), 1707–1720.
Mao, Y., Nijssen, B., Lettenmaier, D.P., 2015. Is climate change implicated in the 2013–2014 California drought? A hydrologic perspective. Geophys. Res. Lett. 42 (8), 2805–2813.
McKee, T.B., Doesken, N.J., Kleist, J., 1993, January. The relationship of drought frequency and duration to time scales. In: Proceedings of the 8th Conference on Applied Climatology. Boston, MA, American Meteorological Society (Vol. 17, No. 22, pp. 179-183).
Medellín-Azuara, J., MacEwan, D., Howitt, R.E., Sumner, D.A., Lund, J.R., Scheer, J., Gailey, R., Hart, Q., Alexander, N.D., Arnold, B., Kwon, A., 2016. Economic Analysis of the 2016 California Drought on Agriculture.
Minnesota IMPLAN Group, 2009. IMPLAN Professional, Version 3.0. IMPLAN Group, Stillwater, MN, USA.
Mishra, V., Cherkauer, K.A., Shukla, S., 2010. Assessment of drought due to historic climate variability and projected future climate change in the midwestern United States. J. Hydrometeorol. 11 (1), 46–68.
Nam, W.H., Hayes, M.J., Svoboda, M.D., Tadesse, T., Wilhite, D.A., 2015. Drought hazard assessment in the context of climate change for South Korea. Agric. Water Manag. 160, 106–117.
Orlowsky, B., Seneviratne, S.I., 2013. Elusive drought: uncertainty in observed trends and short-and long-term CMIP5 projections. Hydrol. Earth Syst. Sci. 17 (5), 1765–1781.
Pauw, K., Thurlow, J., Bachu, M., Van Seventer, D.E., 2011. The economic costs of extreme weather events: a hydrometeorological CGE analysis for Malawi. Environ. Dev. Econ. 16 (2), 177–198.
Peck, D.E., Adams, R.M., 2010. Farm-level impacts of prolonged drought: is a multiyear event more than the sum of its parts? Aust. J. Agric. Resour. Econ. 54 (1), 43–60.
Riahi, K., Rao, S., Krey, V., Cho, C., Chirkov, V., Fischer, G., Kindermann, G., Nakicenovic, N., Rafaj, P., 2011. RCP 8.5-a scenario of comparatively high greenhouse gas emissions. Clim. Chang. 109 (1–2), 33–57.
Riebsame, W.E., Changnon, S.A., Karl, T.R., 1990. Drought and Natural Resource Management in the United States: Impacts and Implications of the 1987–1989 Drought. Westview Press, pp. 174.
Rogelj, J., Meinshausen, M., Knutti, R., 2012. Global warming under old and new scenarios using IPCC climate sensitivity range estimates. Nat. Clim. Chang. 2 (4), 248.
Schlaepfer, D.R., Bradford, J.B., Lauenroth, W.K., Munson, S.M., Tietjen, B., Hall, S.A., Wilson, S.D., Duniway, M.C., Jia, G., Pyke, D.A., Lkhagva, A., 2017. Climate change reduces extent of temperate drylands and intensifies drought in deep soils. Nat. Commun. 8, 14196.
Seager, R., Ting, M., Held, I., Kushnir, Y., Lu, J., Vecchi, G., Huang, H.P., Harnik, N., Leetmaa, A., Lau, N.C., Li, C., 2007. Model projections of an imminent transition to a more arid climate in southwestern North America. Science 316 (5828), 1181–1184.
Sehgal, V., Sridhar, V., Juran, L., Ogejo, J., 2018. Integrating climate forecasts with the soil and water assessment tool (SWAT) for high-resolution hydrologic simulation and forecasts in the Southeastern U.S. Sustain. For. 10, 3079. https://doi.org/10.3390/su10093079.
Sheffield, J., Wood, E.F., 2008. Global trends and variability in soil moisture and drought characteristics, 1950–2000, from observation-driven simulations of the terrestrial hydrologic cycle. J. Clim. 21 (3), 432–458.
Shukla, S., Steinemann, A.C., Lettenmaier, D.P., 2011. Drought monitoring for Washington State: Indicators and applications. J. Hydrometeorol. 12 (1), 66–83.
Sridhar, V., Wedin, D.A., 2009. Hydrological behavior of grasslands of the sandhills: water and energy balance assessment from measurements, treatments and modeling. Ecohydrology 2, 195–212. https://doi.org/10.1002/eco.61.
Sridhar, V., Loope, D.B., Mason, J.A., Swinehart, J.B., Oglesby, R.J., Rowe, C.M., 2006. Large Wind Shift on the Great Plains during the medieval warm period. Science 313 (5785), 345–347. https://doi.org/10.1126/science.1128941.
Svoboda, M., LeComte, D., Hayes, M., Heim, R., Gleason, K., Angel, J., Rippey, B., Tinker, R., Palecki, M., Stooksbury, D., Miskus, D., 2002. The drought monitor. Bull. Am. Meteorol. Soc. 83 (8), 1181–1190.
Thilakarathne, M., Sridhar, V., 2017. Characterization of future drought conditions in the lower Mekong Basin. Weather Climate Extremes 17, 47–58. https://doi.org/10.1016/j.wace.2017.07.004.
Thomson, A.M., Calvin, K.V., Smith, S.J., Kyle, G.P., Volke, A., Patel, P., Delgado-Arias, S., Bond-Lamberty, B., Wise, M.A., Clarke, L.E., et al., 2011. Rcp4. 5: a pathway for stabilization of radiative forcing by 2100. Clim. Chang. 109 (1–2), 77–94.
USDA NASS, 2012. Census of Agriculture, Ag Census Web Maps. Available at: www.agcensus.usda.gov/Publications/2012/Online_Resources/Ag_Census_Web_Maps/Overview/.
Van Vuuren, D.P., Edmonds, J., Kainuma, M., Riahi, K., Thomson, A., Hibbard, K., Hurtt, G.C., Kram, T., Krey, V., Lamarque, J.F., Masui, T., 2011. The representative concentration pathways: an overview. Clim. Chang. 109 (1-2), 5.
VDEM (Virginia Department of Emergency), 2013. Commonwealth of virginia hazard mitigation plan, Chapter 3. In: Hazard Identification and Risk Assessment.
Wang, L., Chen, W., 2014. A CMIP5 multimodel projection of future temperature, precipitation, and climatological drought in China. Int. J. Climatol. 34 (6), 2059–2078.
Wuebbles, D.J., Kunkel, K., Wehner, M., Zobel, Z., 2014. Severe weather in United States under a changing climate. Eos. Trans. AGU 95 (18), 149–150.
Ziolkowska, J.R., 2016. Socio-economic implications of drought in the agricultural sector and the state economy. Economies 4 (3), 19.